Secreted frizzled-related protein 4 is a potent tumor-derived phosphaturic agent

Theresa Berndt, … , Susan C. Schiavi, Rajiv Kumar

Article **Nephrology**

Tumors associated with osteomalacia elaborate the novel factor(s), phosphatonin(s), which causes phosphaturia and hypophosphatemia by cAMP-independent pathways. We show that secreted frizzled-related protein-4 (sFRP-4), a protein highly expressed in such tumors, is a circulating phosphaturic factor that antagonizes renal Wnt-signaling. In cultured opossum renal epithelial cells, sFRP-4 specifically inhibited sodium-dependent phosphate transport. Infusions of sFRP-4 in normal rats over 2 hours specifically increased renal fractional excretion of inorganic phosphate (FE_{Pi}) from 14% ± 2% to 34% ± 5% (mean ± SEM, $P < 0.01$). Urinary cAMP and calcium excretion were unchanged. In thyroparathyroidectomized rats, sFRP-4 increased FE_{Pi} from 0.7% ± 0.2% to 3.8% ± 1.2% $P < 0.05$), demonstrating that sFRP-4 inhibits renal inorganic phosphate reabsorption by PTH-independent mechanisms. Administration of sFRP-4 to intact rats over 8 hours increased FE_{Pi}, decreased serum phosphate (1.95 ± 0.1 to 1.53 ± 0.09 mmol/l$P < 0.05$) but did not alter serum 1α, 25-dihydroxyvitamin D, renal 25-hydroxyvitamin D 1α-hydroxylase cytochrome P450, and sodium-phosphate cotransporter mRNA concentrations. Infusion of sFRP-4 antagonizes Wnt action as demonstrated by reduced renal β-catenin and increased phosphorylated β-catenin concentrations. The sFRP-4 is detectable in normal human serum and in the serum of a patient with tumor-induced osteomalacia. Thus, sFRP-4 displays phosphatonin-like properties, because it is a circulating protein that promotes phosphaturia and hypophosphatemia and blunts compensatory increases in 1α, […]

Find the latest version:

Secreted frizzled-related protein 4 is a potent tumor-derived phosphaturic agent

Theresa Berndt,[1,2] Theodore A. Craig,[1,2] Ann E. Bowe,[5] John Vassiliadis,[5] David Reczek,[5] Richard Finnegan,[5] Suzanne M. Jan De Beur,[4] Susan C. Schiavi,[5,6] and Rajiv Kumar[1,2,3]

[1]Department of Medicine, Nephrology Research Unit,
[2]Mayo Proteomics Research Center, and
[3]Biochemistry and Molecular Biology, Mayo Clinic and Foundation, Rochester, Minnesota, USA
[4]Department of Medicine, Division of Endocrinology, Johns Hopkins University, Baltimore, Maryland, USA
[5]Receptor Ligand Therapeutics and
[6]Renal Sciences Group, Genzyme Corp., One Mountain Road, Framingham, Massachusetts, USA

Tumors associated with osteomalacia elaborate the novel factor(s), phosphatonin(s), which causes phosphaturia and hypophosphatemia by cAMP-independent pathways. We show that secreted frizzled-related protein-4 (sFRP-4), a protein highly expressed in such tumors, is a circulating phosphaturic factor that antagonizes renal Wnt-signaling. In cultured opossum renal epithelial cells, sFRP-4 specifically inhibited sodium-dependent phosphate transport. Infusions of sFRP-4 in normal rats over 2 hours specifically increased renal fractional excretion of inorganic phosphate (FE_{Pi}) from 14% ± 2% to 34% ± 5% (mean ± SEM, $P < 0.01$). Urinary cAMP and calcium excretion were unchanged. In thyro-parathyroidectomized rats, sFRP-4 increased FE_{Pi} from 0.7% ± 0.2% to 3.8% ± 1.2% ($P < 0.05$), demonstrating that sFRP-4 inhibits renal inorganic phosphate reabsorption by PTH-independent mechanisms. Administration of sFRP-4 to intact rats over 8 hours increased FE_{Pi}, decreased serum phosphate (1.95 ± 0.1 to 1.53 ± 0.09 mmol/l, $P < 0.05$) but did not alter serum 1α, 25-dihydroxyvitamin D, renal 25-hydroxyvitamin D 1α-hydroxylase cytochrome P450, and sodium-phosphate cotransporter mRNA concentrations. Infusion of sFRP-4 antagonizes Wnt action as demonstrated by reduced renal β-catenin and increased phosphorylated β-catenin concentrations. The sFRP-4 is detectable in normal human serum and in the serum of a patient with tumor-induced osteomalacia. Thus, sFRP-4 displays phosphatonin-like properties, because it is a circulating protein that promotes phosphaturia and hypophosphatemia and blunts compensatory increases in 1α, 25-dihydroxyvitamin D.

Introduction

Tumor-induced osteomalacia (TIO) is a rare syndrome associated with hypophosphatemia, excessive renal phosphate excretion, osteomalacia, and abnormal vitamin D metabolism (1–8). Tumors associated with this syndrome are usually of mesenchymal origin and are believed to elaborate a circulating factor known as phosphatonin, which is responsible for the syndrome

(1–8). Complete removal of such tumors is associated with remission of the biochemical and skeletal abnormalities. In contrast to hyperparathyroidism and humoral hypercalcemia of malignancy, serum calcium, parathyroid hormone (PTH), and parathyroid hormone–related protein (PTHrP) concentrations are generally normal in TIO (2–5). Serum 1α, 25-dihydroxyvitamin D concentrations, which would be expected to be increased in the presence of hypophosphatemia, are normal or reduced (2–5).

Previously, we showed that a tumor associated with this syndrome secreted a factor (or factors) that had biological properties distinct from those of other known phosphaturic proteins such as PTH and PTHrP (2). Like PTH and PTHrP, tumor supernatants inhibited sodium-dependent phosphate transport, but not sodium-dependent glucose or amino acid transport, in cultured opossum kidney (OK) cells. In contrast to the actions of PTH and PTHrP, which are mediated by 3′, 5′ cAMP, tumor cell supernatants inhibited sodium-dependent phosphate transport without altering cAMP concentrations. The inhibitory effect of tumor supernatants on sodium-dependent phosphate transport was not blocked following treatment with a PTH recep-

tor antagonist, further indicating that the substance present in tumor supernatants was not PTH or PTHrP. This factor was named phosphatonin (9) to distinguish it from other known phosphaturic proteins. These findings have been subsequently confirmed by other investigators (10, 11).

Until recently, the chemical identity of phosphatonin has been elusive. Work by several groups demonstrated that FGF-23 is expressed in tumors associated with TIO (12–15). We and, subsequently, others demonstrated that FGF-23 specifically inhibited phosphate transport in vitro (12, 16). Furthermore, FGF-23 administration or overexpression in animals reproduces the renal phosphate wasting and osteomalacia observed in patients with TIO (16–18). The recent demonstration that some patients with TIO have elevated serum FGF-23 levels (19, 20) further supports the hypothesis that FGF-23 is a phosphatonin.

Coincident with the above studies, we performed serial analysis of gene expression (SAGE) of four tumors associated with renal phosphate wasting to identify the most highly and differentially expressed genes present in such tumors (21). In addition to *FGF-23*, we identified several other genes, including *secreted frizzled-related protein 4* (*sFRP-4*), as phosphatonin candidates. Given that sFRP-4 is a highly and differentially expressed secreted protein with a previously unknown function, we investigated its potential as a phosphatonin.

To test whether sFRP-4 inhibits renal sodium-dependent phosphate transport, we monitored the effect of recombinant sFRP-4 on radiolabeled inorganic phosphorus uptake in renal epithelial cells in vitro, and we intravenously infused recombinant sFRP-4 in rats and mice to assess its effect on solute transport in vivo. We now report that sFRP-4 is a potent phosphate-regulating agent in vitro and in vivo and that it acts independently of PTH. Furthermore, sFRP-4 disrupts the compensatory increase in renal 25-hydroxyvitamin D 1α-hydroxylase cytochrome P450 messenger RNA concentrations and serum 1α, 25-dihydroxyvitamin D concentrations typically observed in response to hypophosphatemia. To determine whether sFRP-4 is indeed a circulating factor, as is characteristic of phosphatonin, we measured and detected sFRP-4 in normal human serum and in the serum of a patient with TIO. Moreover, we demonstrate that sFRP-4 functions as an antagonist of Wnt signaling in the kidney because the administration of sFRP-4 in vivo is associated with a decrease in total β-catenin and an increase in phosphorylated β-catenin in renal tissues. Our data show that sFRP-4 could potentially function as a phosphatonin. Thus, tumors associated with osteomalacia elaborate at least two phosphaturic factors, FGF-23 and sFRP-4.

Methods

Synthesis and purification of sFRP-4. A cDNA pool was synthesized from a TIO tumor using the Lambda ZAP-CMV cDNA synthesis kit (Stratagene, La Jolla, California, USA) (22, 23). Full-length human *sFRP-4* cDNA containing the open reading frame minus the stop codon was amplified from the cDNA pool using the sense primer 5′GCAGTGCCATGTTCCTCTCCATCC3′ and the antisense primer 5′CACTCTTTTCGGGTT-TGTTCTC3′ and high-fidelity *Taq* DNA polymerase (Invitrogen Corp., Carlsbad, California, USA) (22, 23). The amplicon was cloned in frame with the V5-His epitopes into pcDNA3.1-V5-His/TOPO (Invitrogen Corp.) or pIB/V5-His insect vector (Invitrogen Corp.) (22, 23), and the sequence fidelity was confirmed (Sequegen Co., Worcester, Massachusetts, USA). BTI-TN-5B1-4 (High Five) *Trichoplusia ni* insect cells were stably transformed with pIB/V5-His-sFRP-4 and grown in Express Five serum-free medium supplemented with 90 ml of 200 mM L-glutamine per liter (Invitrogen Corp.) and Blasticidin S for selection and maintenance of stock cultures in 75-cm² bottles (Invivogen Inc., San Diego, California, USA). For large-scale expression of sFRP-4, a 2-l Ehrlenmeyer flask containing 0.5 l Express Five medium was inoculated with approximately 0.5×10^6 to 1×10^6 cells/ml and grown at 27°C and 120 rpm in an Innova 4330 temperature-controlled incubator-shaker (New Brunswick Scientific Co. Inc., Edison, New Jersey, USA). Conditioned medium was obtained after 5–6 days of culture growth (final cell density approximately 0.4×10^7 to 1×10^7 cells/ml). Secreted FRP-4 was adsorbed from filtered conditioned medium to 25 ml SP Sepharose resin (Amersham Biosciences, Piscataway, New Jersey, USA) for about 12 hours at 4°C with stirring. The resin was batch washed sequentially four times with each buffer, using 10 vol of 20 mM Na_2HPO_4 (pH 7.4), 65 mM NaCl (start buffer), followed by 20 mM Na_2HPO_4 (pH 7.4), and 200 mM NaCl (intermediate buffer). Secreted FRP-4 was eluted with three washes of 50 ml of 20 mM Na_2HPO_4 (pH 7.4) and 1 M NaCl. The eluate was dialyzed into 500 ml start buffer at 4°C using Spectra/Por 7 dialysis tubing (1,000 molecular-weight cut-off; Spectrum Medical Industries, Laguna Hills, California, USA) with three changes of buffer. The dialysate was filtered (0.2 μm, 25-mm nylon syringe filter; Nalge Co., Rochester, New York, USA) and applied to a Hi Prep 16/10 FF SP Sepharose column using an ÄKTA fast-performance liquid chromatography protein-purification system (Amersham Biosciences). Secreted FRP-4 protein was eluted using a programmed elution gradient starting with 20 mM Na_2HPO_4 (pH 7.4), 65 mM NaCl, and ending with 20 mM Na_2HPO_4 (pH 7.4), 1.0 M NaCl. Fractions containing sFRP-4 were identified by anti-V5 immunoblot analysis, concentrated using Centriprep 10 (Amicon, Beverly, Massachusetts, USA) and sterile filtered using 0.2-μm nylon syringe filters. Secreted FRP-4 protein had the expected N-terminal amino acid sequence (APC/XEAV).

Effect of sFRP-4 on phosphate transport in OK cells. OK cells were cultured in 45% DMEM, 45% F12 medium, with 10% FCS. The cells were seeded at a density of about 5×10^3 per well in 24-well tissue-culture plates

and sodium-dependent phosphate, alanine, and glucose cotransport measured as described previously (2, 12). In brief, sFRP-4 or vehicle was added in varying amounts to growth medium to attain concentrations shown in Figure 1. For the measurement of sodium-dependent phosphate transport, 0.1 mM dibasic potassium phosphate was included in the transport medium, and ^{32}P dibasic potassium phosphate was added to a final specific activity of 2 μCi/ml. For sodium-dependent alanine transport, 0.1 mM L-alanine and ^{3}H-alanine were added (final specific activity, 1 μCi/ml). For glucose transport, 0.1 mM methyl-α-glucopyranoside and methyl (α-d-[^{14}C] gluco) pyranoside were added (final specific activity, 0.2 μCi/ml). The transport of phosphate, alanine, and methyl-α-glucopyranoside were assayed separately. Each transport reaction was measured in three or four duplicate wells and each assay included control blank wells to correct for solute bound to cell surfaces, intracellular spaces, and culture dish.

Animals. All animal protocols were approved by the Institutional Animal Care and Use Committee of the Mayo Clinic. Male Sprague-Dawley rats weighing 250–300 g were purchased from Harlan Sprague Dawley Inc. (Madison, Wisconsin, USA). They were fed a standard rodent formula containing 0.7% phosphorus and 0.5% calcium and adequate amounts of vitamin D. On the day of the acute experiments, rats were anesthetized with an intraperitoneal injection of 100–150 mg/kg body weight of 5-sec-butyl-ethyl-2-thiobarbituric acid (inactin; Byk Gulden Konstanz, Hamburg, Germany). The animals were placed on a heated table to maintain body temperature between 36°C and 38°C. After a tracheostomy, a PE-50 catheter was placed in the left carotid artery to monitor mean arterial blood pressure (MAP) and to collect blood samples. Another catheter was placed in the left jugular vein for intravenous infusion of 1% inulin in 0.9% NaCl and 2.25% BSA at a rate of 1% per body weight per hour and for drug administration. A PE-90 catheter was placed in the bladder for urine collection. The groups of animals studied were as discussed next.

Short-term (2-hour) infusion of vehicle (group 1, n = 7) or sFRP-4 (group 2, n = 10) and the effects on solute excretion in normal rats. After a 1.5-hour recovery period, one 30-minute urine clearance sample was taken (C_1), and approximately 35 μl of vehicle containing PBS and 0.1% BSA (group 1) or sFRP-4 in vehicle (group 2; 0.3 μg/kg/h of sFRP-4) was added to the inulin/BSA infusion. After a 45-minute stabilization period, a 60-minute urine clearance (C_2) was taken from either vehicle-treated or sFRP-4–treated animals. A blood sample was taken at the midpoint of the clearance period. At the end of the experiment, the kidneys were removed for isolation of total RNA and quantitation of 25-hydroxyvitamin D 1α-hydroxylase and 25-hydroxyvitamin D 24-hydroxylase cytochrome P450 mRNAs.

Short-term (2-hour) infusion of vehicle (group 3, n = 6) or sFRP-4 (group 4, n = 10) and the effect on solute excretion in thyro-parathyroidectomized rats. These protocols are iden-

tical to those described for groups 1 and 2, except that thyro-parathyroidectomized (TPTX) rats were studied 2 hours after the completion of thyro-parathyroidectomy. Effective thyro-parathyroidectomy was confirmed by a significant reduction in the urinary fractional excretion of phosphate, increased fractional excretion of calcium, and the presence of hypocalcemia.

Long-term (8-hour) infusion of vehicle (group 5, n = 5) or sFRP-4 (group 6, n = 7) and the effects on solute excretion, serum 1,25-dihydroxyvitamin D concentrations, and 25-hydroxyvitamin D 1α-hydroxylase cytochrome P450 and 25-hydroxyvitamin D 24-hydroxylase cytochrome P450 mRNA concentrations. These protocols are identical to those described for the previous groups, except that after the control collection (C_1), 1 hour clearances were taken at 4 hours (C_2) and 7 hours (C_3) after initiation of the vehicle or sFRP-4 infusions. At the end of the experiment, blood was collected for measurement of 1α, 25-dihydroxyvitamin D, and kidneys were collected for the isolation of mRNA and assessment of 25-hydroxyvitamin D 1α-hydroxylase cytochrome P450 and 25-hydroxyvitamin D 24-hydroxylase cytochrome P450 mRNA concentrations by quantitative real-time RT-PCR. To determine if decrements in serum phosphate were associated with appropriate increases in renal 25-hydroxyvitamin D 1α-hydroxylase cytochrome P450 mRNA concentrations, rats were maintained on a 0.1% phosphate diet (low Pi) or a 0.4% phosphate diet (normal Pi) for a period of 1 week, so as to bring about a modest reduction in serum phosphate equivalent to that seen following sFRP-4 infusion.

Serum and urine measurements. Serum and urinary phosphate concentrations were determined using the method of Chen et al. (24). Serum and urine inulin concentrations were measured using the anthrone method (25). Sodium concentrations were measured in urine using an Instrumentation Laboratory flame photometer (Instrumentation Laboratory, Wilmington, Massachusetts, USA). Serum and urine calcium concentrations were determined by atomic absorption spectrometry (26–29). Plasma 1α, 25-dihydroxyvitamin D and 25-hydroxyvitamin D concentrations were measured by
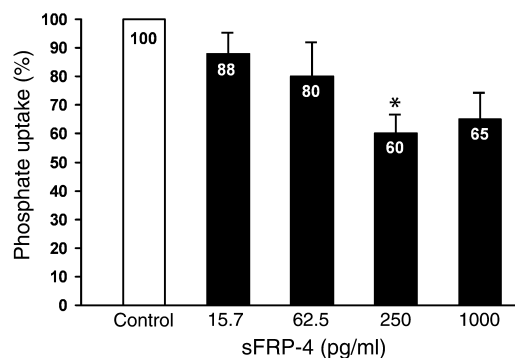
Figure 1
Effect of sFRP-4 on sodium-dependent phosphate uptake in OK cells maintained in culture. *$P < 0.05$.

radio immunoassay (Diasorin Inc., Stillwater, Minnesota, USA). Urinary cyclic adenosine monophosphate was measured using an enzyme immunoassay (Amersham Biosciences).

Real-time PCR to assess 25-hydroxyvitamin D 1α-hydroxylase cytochrome P450 and 25-hydroxyvitamin D 24-hydroxylase cytochrome P450 messenger RNA concentrations in the kidney. A Polytron (Brinkman Instruments, Westbury, New York, USA) was used to homogenize a lateral third of each rat kidney containing cortical tissue in 4 ml of RLT buffer (QIAGEN Inc., Valencia, California, USA). The homogenate was centrifuged for 3 minutes at 4,500 g. Total RNA was extracted from the supernatant following treatment with DNase using the RNeasy midi kit (QIAGEN Inc.). RNA concentration in the samples was quantitated using UV spectroscopy at a wavelength of 260 nm. Samples containing 200 ng total RNA were prepared using the Quantitect SYBR Green RT-PCR kit (QIAGEN Inc.) and real-time PCR done following the manufacturer's protocol on a PE Applied Biosystems model 7700 sequence detector (PE Applied Biosystems, Foster City, California, USA). Primers were designed to span introns and to generate amplicons of 100–120 bp. The primer sequences are as follows: 25-hydroxyvitamin D 1α-hydroxylase cytochrome P450 (forward, 5′GCAT CCATCTCCAGTTTGTAGAC3′; reverse, 5′TGTGCCTCTTGTGCATAGTAAGA3′); 25-hydroxyvitamin D 24-hydroxylase cytochrome P450 (forward, 5′GATCACCTTTCCAAGAAGGAACT3′; reverse, 5′AGAGAATCCACATCAAGCTGTTC3′); and sodium-dependent phosphate cotransporter IIa (forward, 5′CTGTGCACTTGTCTTATCCTCCT3′; reverse 5′GGAA-GTCTGTGTTGATGACCTT3′). Long oligonucleotide templates were designed that represented the entire amplicon sequence for each gene, dilutions of which were used to generate standard curves. All samples were interrogated in triplicate, and the averages of each normalized to GAPDH. GAPDH mRNA values did not deviate significantly across samples. Normalized relative values were assigned absolute values based on the slope and y intercept of the relevant standard curve. All PCR products, including reverse-transcriptase negative control, and no template control samples were subjected to electrophoresis on a 4% agarose gel. Only expected band sizes were detected.

ELISA for sFRP-4 in serum. A two-Ab sandwich ELISA was developed using mAb's (mAb's 3.1 and 3.4) against insect-derived sFRP-4 protein. These Ab's were prepared in the Mayo Clinic Core Facility using established procedures (30). Briefly, mAb 3.4 was immobilized onto a Reacti-Bind ELISA plate (Pierce Chemical Co., Rockford, Illinois, USA). Recombinant sFRP-4 standards in 100 μl of PBS or 100 μl human serum samples were added to individual wells and incubated at room temperature for 1 hour. Samples were aspirated and wells washed three times with PBS and 0.5% Tween-20. A second anti–sFRP-4 mAb, mAb 3.1, was biotinylated with sulfo-NHS-LC-biotin (Pierce Chemical Co.), applied to each well, and incubated for 1 hour at room temperature. Samples were aspirated and wells washed three times with PBS and 0.5% Tween-20. Streptavidin-HRP (100 ng/ml) (Pierce Chemical Co.) was added to facilitate detection with 3,3,5,5 tetramethylbenzidine substrate (Sigma-Aldrich, St. Louis, Missouri, USA). After the addition of stop solution (Alpha Diagnostic International Inc., San Antonio, Texas, USA), the plate was read in a SpectraMax Plus spectrophotometer (Molecular Devices Corp., Sunnyvale, California, USA) at 450 nm. The concentration of sFRP-4 in each serum sample was calculated based on a standard curve generated using known concentrations of purified insect sFRP-4.

Western blotting to detect β-catenin and phosphorylated β-catenin or sFRP-4 in renal tissues. Kidneys (approximately 1 g tissue) from rats infused with sFRP-4 or vehicle, as described above, were homogenized in an equal volume of buffer (50 mM Tris, pH 7.8, 150 mM sodium chloride) containing a mammalian protease inhibitor mixture (P8340; Sigma-Aldrich) and phosphatase inhibitors okadaic acid (1 μM) and microcystin LR (1 μM; Sigma-Aldrich). Equal amounts of protein from control and experimental kidneys were loaded and electrophoresed on SDS-polyacrylamide gels (31). The electrophoresed proteins were transferred to polyvinylidene difluoride membranes (32), and the membranes were probed with Ab's against β-catenin or phosphorylated β-catenin (Cell Signaling Technologies, Beverly, Massachusetts, USA). HRP-conjugated secondary Ab's were used to detect primary Ab's bound to either β-catenin or phosphorylated β-catenin.

For detection of sFRP-4 in renal tissues, rat renal tissue homogenates were electrophoresed on SDS-polyacrylamide gels, and the electrophoresed proteins were transferred to PVDF membranes as described above (31, 32). The mAb's raised against sFRP-4 were used to probe PVDF membranes, and bound anti–sFRP-4 Ab's were detected using an anti–mouse IgG, HRP-coupled Ab.

Statistics. Values are expressed as means plus or minus SE. Statistical comparisons for groups 1–4 were made using a paired t test. Comparisons between multiple clearances (groups 5 and 6) were made using one-way ANOVA followed by the Fisher protected least-significant difference test. Statistical comparison for the phosphate-uptake assay was made using an unpaired t test. A P value less than 0.05 was considered to be significant.

Results

Secreted FRP-4 specifically inhibits sodium-dependent phosphate transport in OK cells. To determine whether sFRP-4 directly inhibits sodium-dependent phosphate transport in OK cells maintained in culture, we added increasing amounts of sFRP-4 to the supernatants of these cells (Figure 1). As can be seen, a dose of 250 pg/ml of sFRP-4 per well caused a statistically significant decrease in sodium-dependent phosphate uptake in OK cells maintained in culture. Sodium-dependent glucose transport (sFRP-4, 10.26 ± 0.33 nmol/mg protein, versus vehicle, 9.62 ± 0.45 nmol/mg
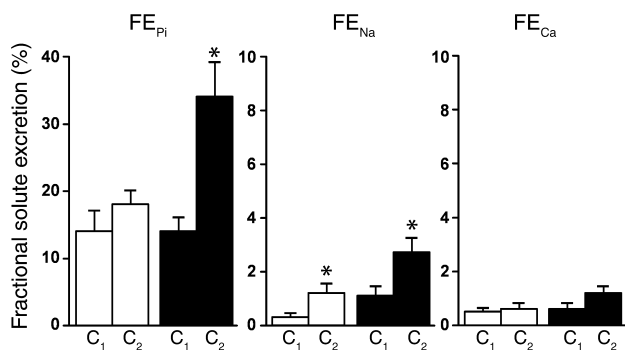
Figure 2

Effect of the infusion of sFRP-4 on solute excretion in intact rats. Intact rats were administered sFRP-4 (black bars; group 2) at a dose of 0.3 μg/kg/h or vehicle (white bars; group 1) by intravenous infusion over a period of 2 hours. C_1 indicates equilibration period prior to the infusion of sFRP-4 or vehicle. C_2 indicates experimental period during which sFRP-4 or vehicle was infused. Fractional excretion of inorganic phosphate, sodium, and calcium were measured as described in the text. *$P < 0.05$.

protein; P = NS) and sodium-dependent alanine transport (sFRP-4, 0.059 ± 0.008 nmol/mg protein, versus vehicle, 0.083 ± 0.009 nmol/mg protein; P = NS) did not change significantly.

Effects of short-term sFRP-4 infusion on renal solute transport, renal 25-hydroxyvitamin D 1α-hydroxylase mRNA, and 25-hydroxyvitamin D 24-hydroxylase mRNA. As shown in Figure 2, sFRP-4 infused in normal rats over a period of 2 hours caused a marked increase in the fractional excretion of phosphate (FE_{Pi}) from 14% ± 2% to 34% ± 5%, mean ± SEM; $P < 0.05$. FE_{Pi} was stable (14% ± 3% to 18% ± 2%, mean ± SEM; P = NS) in vehicle-infused rats. Fractional sodium excretion (FE_{Na}) increased in the sFRP-4–infused rats from 1.1% ± 0.3% to 2.7% ± 0.5% (mean ± SEM; $P < 0.05$). In the vehicle-infused group, a smaller increase in FE_{Na} was noted (0.3% ± 0.1% to 1.2% ± 0.3%, mean ± SEM; $P < 0.05$). Fractional excretion of calcium (FE_{Ca}) did not change in either group. GFR and MAP were stable in both groups of animals (data not shown). Of note, urinary cAMP excretion did not change in either the sFRP-4–infused (23.6 ± 2.6 to 25.5 ± 2.6 nmol/min; P = NS) or vehicle-infused (24.6 ± 1.2 to 28.2 ± 3.5 nmol/min; P = NS) groups of rats. Serum phosphate and serum calcium concentrations did not change during the short-term infusion in the sFRP-4. Renal 25-hydroxyvitamin D 1α-hydroxylase cytochrome P450 mRNA (sFRP-4, 2.29 × 10⁻¹³ ± 1.18 × 10⁻¹³ mol/pg RNA, versus vehicle, 4.36 × 10⁻¹³ ± 1.82 × 10⁻¹³ mol/pg RNA; P = NS) and 24-hydroxylase cytochrome P450 mRNA (sFRP-4, 3.73 × 10⁻¹⁴ ± 1.35 × 10⁻¹⁴, versus vehicle, 1.45 × 10⁻¹⁴ ± 4.0 × 10⁻¹⁵ mol/pg RNA; P = NS) concentrations were similar in the sFRP-4 and vehicle-treated groups.

Parallel experiments in mice were also performed using recombinant protein derived from mammalian or insect cells. Secreted FRP-4 also induced a 3.1-fold

increase in the FE_{Pi} in mice ($P < 0.05$). These results confirm the actions of sFRP-4 in another species and demonstrate that the method of production of recombinant sFRP-4 (mammalian versus insect expression systems) has no major influence on protein function.

The phosphaturic action of sFRP-4 is PTH independent. To determine whether PTH is necessary for the phosphaturic action of sFRP-4, we infused sFRP-4 intravenously in acutely TPTX rats. Thyro-parathyroidectomy was associated with a decrease in the basal FE_{Pi} from approximately 15% in intact animals to approximately 0.7% in TPTX animals. Basal FE_{Ca} increased from 0.5% to 1.5%, and serum calcium decreased from approximately 10.5 mg/dl to 8 mg/dl. As shown in Figure 3, sFRP-4 infusion in acutely TPTX animals was associated with a 3.5-fold increase in the FE_{Pi} (1.0% ± 0.3% to 3.8% ± 1.2%; $P < 0.05$). This 3.5-fold increase during sFRP-4 infusion was similar to that observed in intact animals. The FE_{Pi} was stable in animals receiving the vehicle. There were no changes in the fractional excretion of sodium or calcium in rats infused with sFRP-4. GFR and MAP were stable throughout the experiment.

Long-term sFRP-4 infusion results in increased fractional excretion of phosphorus, reduced serum phosphorus concentrations, and inappropriately normal serum 1α, 25-dihydroxyvitamin D concentrations. We examined the effects of a long-term (8 hour) infusion of sFRP-4 on fractional excretion of solutes, serum inorganic phosphorus, serum 1,25-dihydroxyvitamin D concentrations, and renal 25-hydroxyvitamin D 1α-hydroxylase cytochrome P450 and 25-hydroxyvitamin D 24-hydroxylase cytochrome P450 messenger RNA concentrations. With long-term infusion of sFRP-4 (Table 1), FE_{Pi} increased from 8.5% ± 2.6% to 20.2% ± 3.7% 4 hours after initiation of sFRP-4 infusion and was 18.2% ± 4.3% at 8 hours. FE_{Pi} did not change in the animals infused with vehicle. There were no changes
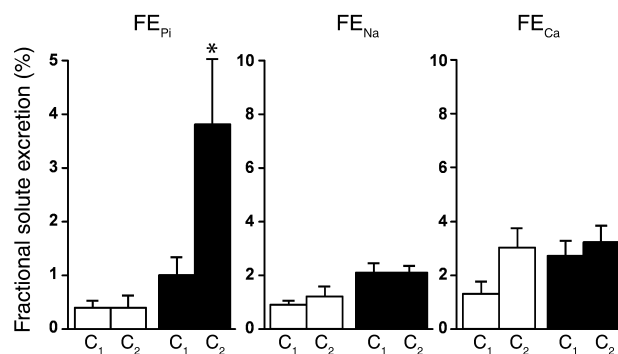
Figure 3

Effect of the infusion of sFRP-4 on solute excretion in TPTX rats. TPTX rats were administered sFRP-4 (black bars; group 4) at a dose of 0.3 μg/kg/h or vehicle (white bars; group 3) by intravenous infusion over a period of 2 hours. C_1 indicates collection period prior to the infusion of sFRP-4 or vehicle. C_2 indicates collection period during which sFRP-4 or vehicle was infused. Fractional excretion of inorganic phosphate, sodium, and calcium were measured as described in the text. *$P < 0.05$.

Table 1
Effect of long-term (8 hour) infusion of sFRP-4 on renal function in intact rats

|	Vehicle ($n = 5$)			sFRP-4 ($n = 7$)		
	C_1	C_2	C_3	C_1	C_2	C_3
GFR ± SE (ml/min)	3.7 ± 0.6	3.2 ± 0.4	2.6 ± 0.6	3.5 ± 0.2	2.8 ± 0.3	2.4 ± 0.5
FE_{Pi} ± SE (%)	7.4 ± 2.2	6.8 ± 1.7	9.9 ± 0.4	8.5 ± 2.6	20.2 ± 3.7[A]	18.2 ± 4.3
FE_{Na} ± SE (%)	1.6 ± 0.4	1.3 ± 0.2	0.8 ± 0.1	1.9 ± 0.6	1.8 ± 0.2	2.2 ± 1.1
FE_{Ca} ± SE (%)	0.8 ± 0.2	0.8 ± 0.2	0.8 ± 0.2	0.9 ± 0.3	0.8 ± 0.1	0.7 ± 0.3
P_{Pi} ± SE (mM)	2.02 ± 0.15	2.02 ± 0.22	1.83 ± 0.18	1.95 ± 0.10	1.51 ± 0.11[A]	1.53 ± 0.09[A]
P_{Ca} ± SE (mg/dl)	8.0 ± 0.3	9.1 ± 0.3	8.8 ± 0.6	8.7 ± 0.7	9.1 ± 0.3	9.7 ± 0.5
MAP ± SE (mmHg)	119 ± 6	113 ± 8	108 ± 5	124 ± 10	118 ± 7	120 ± 6
Serum 1α, 25(OH)$_2$D (pg/ml)		62.4 ± 29.2			88.9 ± 26.8	
Renal 25(OH)D 1α-hydroxylase cytochrome P450 mRNA (mol/pg)		$1.41 \times 10^{-13} \pm 3.87 \times 10^{-14}$			$1.37 \times 10^{-13} \pm 1.77 \times 10^{-14}$	
Renal 25(OH)D 24-hydroxylase cytochrome P450 mRNA (mol/pg)		$1.53 \times 10^{-14} \pm 1.38 \times 10^{-15}$			$0.92 \times 10^{-14} \pm 2.48 \times 10^{-15}$	

[A]Indicates a significant difference, ANOVA, $P < 0.05$. P_{Pi}, plasma phosphate concentration; P_{Ca}, plasma calcium concentration. 1α, 25(OH)$_2$D; 1α, 25-dihydroxyvitamin D.

in the fractional excretion of sodium or the fractional excretion of calcium in either the sFRP-4 or vehicle groups. In the sFRP-4–infused animals, there was a decrease in serum phosphorus concentrations from 1.95 ± 1.0 mmol/l to 1.51 ± 0.11 mmol/l at 4 hours and to 1.53 ± 0.09 mmol/l at 8 hours. There was no change in the serum phosphorus concentrations in the animals receiving vehicle. Serum 1α, 25-dihydroxy-vitamin D concentrations were not different between the sFRP-4 and vehicle-infused rats (89.6 ± 26.8 pg/ml for the sFRP-4 group versus 62.4 ± 29.2 pg/ml for the vehicle group, mean ± SEM; P = NS). Concentrations of 25-hydroxyvitamin D 1α-hydroxylase cytochrome P450 messenger mRNA were similar in the vehicle and sFRP-4–infused groups at 8 hours ($1.41 \times 10^{-13} \pm 3.87 \times 10^{-14}$ mol/pg RNA versus $1.37 \times 10^{-13} \pm 1.77 \times 10^{-14}$ mol/pg RNA; P = NS; Figure 4). Concentrations of 25-hydroxyvitamin D 24-hydroxylase cytochrome P450 mRNA showed a tendency to increase in sFRP-4–infused rats, but this value was not statistically significant. In phosphate-deprived rats, renal 25-hydroxyvitamin D 1α-hydroxylase cytochrome P450 messenger mRNA concentrations were appropriately increased approximately 3.7-fold ($8.5 \times 10^{-13} \pm 9.5 \times 10^{-14}$ mol/pg RNA in phosphate-deprived rats, n = 6, versus $2.3 \times 10^{-13} \pm 8.9 \times 10^{-14}$ mol/pg RNA in normal rats, n = 6; P < 0.05; Figure 4) following an approximate 16% decrease in serum Pi and an approximate 33% decrease in urinary phosphate excretion.

The phosphaturic action of sFRP-4 is not mediated through transcriptional regulation of the sodium-dependent phosphate cotransporter. We measured sodium-dependent phosphate cotransporter mRNA concentrations in sFRP-4–treated rats and found that they did not change significantly with sFRP-4 treatment (sFRP-4, $6.93 \times 10^{-11} \pm 6.41 \times 10^{-12}$ mol/pg RNA, versus vehicle, $8.67 \times 10^{-11} \pm 9.20 \times 10^{-12}$ mol/pg RNA).

The protein sFRP-4 is detectable in normal human serum and in the serum of a patient with TIO. We measured sFRP-4 concentrations in normal human serum obtained from five normal subjects. The mean concentration was 34.8 ± 13.3 ng/ml and the range was 5.5–79.8 ng/ml. In a patient with TIO, treated with phosphate and 1α, 25-dihydroxyvitamin D₃, serum sFRP-4 was 11.1 ng/ml.

The protein sFRP-4 is expressed in the rat kidney and antagonizes Wnt signaling. Immunoblot analysis of rat renal homogenates using a monoclonal anti–sFRP-4 Ab indi-
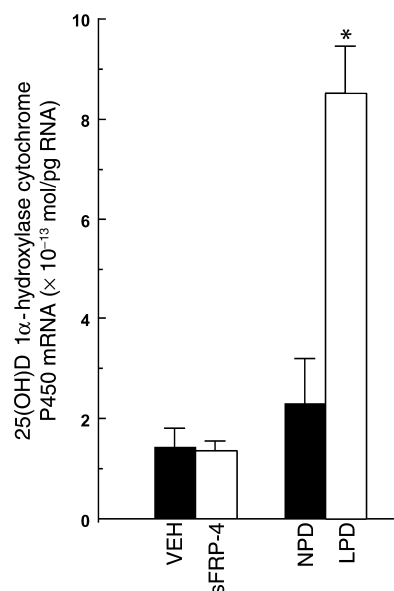
Figure 4
The effect infusion of vehicle (VEH) or sFRP-4 (0.3 μg/kg/h) for 8 hours, or the effect of phosphate deprivation induced by a low-phosphate diet phosphate (LPD) compared with a normal-phosphate diet (NPD), on the concentration of 25-hydroxyvitamin D 1α-hydroxylase cytochrome P450 mRNA concentrations in kidney. *P < 0.05. 25(OH)D, 25-hydroxyvitamin D.
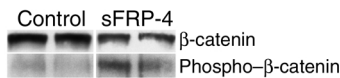
Figure 5
Western blots of renal homogenates obtained from rats infused with vehicle (control) or sFRP-4 for 8 hours. Ab's against β-catenin (upper panel) or phosphorylated β-catenin (phospho β-catenin) (lower panel) were used to detect proteins as described in Methods.

cates that sFRP-4 protein (approximately 50,000 M_r) is detectable in kidney homogenates (data not shown). To determine the mechanism of action of sFRP-4 in the kidney, we measured β-catenin or phosphorylated β-catenin concentrations in sFRP-4– or vehicle –treated kidneys in vivo. As shown in Figure 5, rats infused with sFRP-4 have reduced amounts of renal β-catenin protein (upper panel) and increased phosphorylated β-catenin signal (lower panel) compared with those infused with vehicle.

Discussion

TIO is a paraneoplastic renal phosphate wasting disorder characterized by hypophosphatemia, phosphaturia, and inappropriately normal or low serum 1α, 25-dihydroxyvitamin D concentrations that lead to osteomalacia or rickets, muscle weakness, and general debility (1–8). In TIO, serum calcium, PTH, and PTHrP concentrations are generally normal. The mesenchymal tumors that cause TIO are thought to elaborate a circulating factor that causes the metabolic abnormalities noted above (1–8). Complete removal of the tumors is associated with correction of the biochemical and skeletal abnormalities.

Earlier, we demonstrated that a tumor associated with this syndrome elaborated novel factor(s) responsible for the reduced renal reabsorption of phosphate (2). Recent work suggests that FGF-23 is a phosphatonin-like molecule. In addition to its expression in tumors associated with osteomalacia (13, 15, 33), FGF-23 serum levels are increased in some patients with TIO and X-linked hypophosphatemic rickets (XLH) (19), a syndrome that has phenotypic features similar to TIO (34). Elevated FGF-23 concentrations in the serum of patients with TIO diminish after removal of the tumor and a return of the clinical state to normal (19). FGF-23 reduces phosphate uptake in OK cells in culture (12, 35) and may be a substrate for the enzyme PHEX (12), which is mutated in patients with XLH (36). Shimada et al. showed that recombinant FGF-23 reduces serum phosphate concentrations and increases urinary phosphate losses when administered to mice (13). Furthermore, nude mice implanted with an established cell line expressing FGF-23 develop osteomalacia. Transgenic mice overexpressing FGF-23 have hypophosphatemia and increased urinary phosphate excretion (37), and null-mutant mice lacking the *FGF-23* gene are hyperphosphatemic (38). Finally, activating mutations of FGF-23 are responsible for autosomal dominant hypophosphatemic rickets (ADHR) (17, 39, 40), which also has clinical features similar to TIO and XLH. ADHR mutations have been associated with increased FGF-23 protein stability and/or activity (16–18, 40).

Our approach in identifying potential phosphatonin candidates was to perform a comprehensive gene expression profile in four tumors associated with phosphate wasting and to compare these profiles with those of similar mesenchymal tumors not associated with TIO. We examined several tumors associated with the syndrome of TIO for the presence of differentially expressed genes using the SAGE technique (21, 41, 42). We identified several genes that were expressed preferentially in tumors associated with osteomalacia but not in control tissues. These included *FGF-23, MEPE, dentin matrix protein 1*, and secreted *FRP-4*. Since sFRP-4 is a secreted molecule, we hypothesized that this protein could enter the circulation and reduce phosphate reabsorption in the kidney. To test this hypothesis, we biosynthesized sFRP-4 and demonstrated that it specifically inhibited sodium-dependent phosphate uptake in cultured opossum renal epithelia (Figure 1). Furthermore, we showed that the infusion of sFRP-4 into rats is associated with a 2.5- to threefold increase in the urinary excretion of phosphate (Figure 2, Table 1). In acute experiments, there is an increase in sodium excretion, which is probably secondary to the infusion itself and is independent of sFRP-4 since it is not apparent in animals infused with sFRP-4 for a period of 8 hours. Urinary fractional excretion of calcium and urinary cAMP excretion do not change. The infusion of sFRP-4 for a period of 4–8 hours was associated with a decrease in serum phosphate concentrations. Thus, this protein is capable of causing hyperphosphaturia and hypophosphatemia in vivo.

To determine whether the phosphaturic effects of sFRP-4 are PTH dependent, we infused sFRP-4 into acutely TPTX rats and showed that there was a threefold increase in phosphate excretion (Figure 3). This is similar to the change in FE_{Pi} observed in the intact animal, suggesting that sFRP-4 does not act via PTH-dependent pathways. The maximal absolute increase in FE_{Pi} was less in TPTX rats than in rats with intact parathyroid glands, most likely due to enhanced phosphate reabsorption by the proximal straight tubule in the hypoparathyroid state (43, 44). Further evidence that the phosphaturic effect of sFRP-4 is not PTH dependent comes from the lack of stimulation of urinary cyclic AMP following sFRP-4 infusion in intact rats. The effect of sFRP-4 observed in OK cells maintained in culture further suggests that sFRP-4 has direct actions on Pi transport.

Infusion of sFRP-4 produces the same defect in vitamin D metabolism observed in TIO. Despite the induction of hypophosphatemia following sFRP-4 infusion, serum 1α, 25-dihydroxyvitamin D concentrations and renal 25-hydroxyvitamin D 1α-hydroxylase cytochrome P450 messenger RNA amounts fail to increase in the

predicted physiological manner (Table 1) (45–50). In contrast, phosphate deprivation in normal rats that was associated with mild hypophosphatemia resulted in a significant (3.7-fold) increase in renal 25-hydroxyvitamin D 1α-hydroxylase cytochrome P450 messenger RNA concentrations. This failure of the vitamin D-endocrine system to respond to hypophosphatemic stimuli is characteristic of TIO and the phenotypically related XLH and ADHR (3–5, 51).

We show that sFRP-4 circulates in the serum of normal humans, suggesting that it could potentially function as a phosphatonin. sFRP-4 was also detectable in the serum of a patient with TIO, who had an unresectable tumor and was on treatment with phosphate supplementation and 1α, 25-dihydroxyvitamin D₃. The sFRP-4 concentrations were not elevated relative to the control concentrations. It is possible that treatment of the patient with phosphate and 1α, 25-dihydroxyvitamin D₃ could have suppressed sFRP-4 concentrations. A more comprehensive study of other patients with TIO will be needed prior to making a conclusive statement regarding the usefulness of sFRP-4 concentrations in the diagnosis of TIO. It is of interest that not all patients with TIO have elevations of FGF23, and in some instances cure of the syndrome occurs without changes in FGF-23 concentrations (20).

Sodium-dependent phosphate cotransporter mRNA levels were unchanged following infusion of sFRP-4 in rats. This suggests that transcriptional regulation of sodium-phosphate cotransporter mRNA concentrations by sFRP-4 is not critical in modulating phosphate transport. Others have shown that parathyroid hormone does not alter sodium-phosphate cotransporter mRNA concentrations in the kidney but causes a redistribution in the sodium-phosphate cotransporter protein from the luminal membrane of the proximal tubular cell into the lysosomal compartment (52–54). Preliminary data suggest that sFRP-4 also causes a redistribution of sodium-dependent phosphate cotransporter IIa protein in OK cells (data not shown). Further experiments will be needed to define precisely the effects of sFRP-4 on sodium-dependent phosphate cotransporter IIa protein cell biology.

Our data point to a novel function of sFRP-4 in the kidney. Protein sFRP-4 belongs to a family of secreted proteins that contain a cysteine-rich domain homologous to the extracellular domain of the Wnt receptors, the frizzled proteins (55–59). The sFRPs modulate the activities of Wnts (60–68). The Wnt-signaling pathway plays an important role in renal, bone, and cardiac development (69–77). Binding of Wnts to frizzled receptors leads to activation of signals through three different pathways, resulting in both transcription and nontranscriptional changes (74–78). The sFRP-4 mRNA is detectable in the kidney (58, 79, 80), and these data are supported by our observations that sFRP-4 protein is also detectable in homogenates of rat kidney. We show that sFRP-4 antagonizes Wnt-signaling in the kidney. The binding of Wnts to frizzled receptors normally stabilizes intracellular β-catenin by preventing degradation and decreases the phosphorylation of β-catenin (58, 81–83). Increased phosphorylation of β-catenin suggests that sFRP-4 antagonizes this pathway.

Our findings add to the list of functions attributed to sFRP-4. Expression of sFRP-4 has been correlated with the presence of apoptosis in several tissues such as osteoarthritic cartilage, but colocalization of sFRP-4 in apoptotic cells and direct induction of apoptosis by sFRP-4 has not been demonstrated (80, 84, 85). It is also noteworthy that elevated sFRP-4 expression is correlated with several tumor types and proliferative tissues (86, 87). Based on these observations and the diverse expression pattern of sFRP-4, it is likely that additional functions will be identified (88).

In conclusion, we have shown that a protein that is overexpressed in tumors associated with renal phosphate wasting and osteomalacia is capable of specifically inhibiting sodium-dependent phosphate transport in vitro and selectively increasing the fractional excretion of phosphorus in a PTH-independent manner in vivo. We also show that there is a decrease in serum phosphate concentrations in rats administered this protein for a period of 4–8 hours and that the vitamin D endocrine system fails to respond to hypophosphatemic stimuli following sFRP-4 infusion. Secreted FRP-4 could potentially function as a phosphatonin, and it is apparent from these studies that there are at least two phosphaturic proteins (FGF-23 and sFRP-4) produced by tumors associated with renal phosphate wasting and osteomalacia.

1. Aschinberg, L.C., Solomon, L.M., Zeis, P.M., Justice, P., and Rosenthal, I.M. 1977. Vitamin D-resistant rickets associated with epidermal nevus syndrome: demonstration of a phosphaturic substance in the dermal lesions. *J. Pediatr.* **91**:56–60.
2. Cai, Q., et al. 1994. Brief report: inhibition of renal phosphate transport by a tumor product in a patient with oncogenic osteomalacia. *N. Engl. J. Med.* **330**:1645–1649.
3. Kumar, R. 2000. Tumor-induced osteomalacia and the regulation of phosphate homeostasis. *Bone.* **27**:333–338.
4. Kumar, R. 1997. Phosphatonin—a new phosphaturetic hormone? (lessons from tumour-induced osteomalacia and X-linked hypophosphataemia). *Nephrol. Dial. Transplant.* **12**:11–13.
5. Kumar, R. 2002. New insights into phosphate homeostasis: fibroblast growth factor 23 and frizzled-related protein-4 are phosphaturic factors derived from tumors associated with osteomalacia. *Curr. Opin. Nephrol. Hypertens.* **11**:547–553.
6. Schiavi, S.C., and Moe, O.W. 2002. Phosphatonins: a new class of phosphate-regulating proteins. *Curr. Opin. Nephrol. Hypertens.* **11**:423–430.
7. Stone, E., Bernier, V., Rabinovich, S., and From, G.L. 1984. Oncogenic osteomalacia associated with a mesenchymal chondrosarcoma. *Clin. Invest. Med.* **7**:179–185.
8. Ryan, E.A., and Reiss, E. 1984. Oncogenous osteomalacia. Review of the world literature of 42 cases and report of two new cases. *Am. J. Med.* **77**:501–512.
9. Econs, M.J., and Drezner, M.K. 1994. Tumor-induced osteomalacia—unveiling a new hormone. *N. Engl. J. Med.* **330**:1679–1681.

10. Nelson, A.E., et al. 1996. Characteristics of tumor cell bioactivity in oncogenic osteomalacia. *Mol. Cell Endocrinol.* **124**:17–23.

11. Wilkins, G.E., et al. 1995. Oncogenic osteomalacia: evidence for a humoral phosphaturic factor. *J. Clin. Endocrinol. Metab.* **80**:1628–1634.

12. Bowe, A.E., et al. 2001. FGF-23 inhibits renal tubular phosphate transport and is a PHEX substrate. *Biochem. Biophys. Res. Commun.* **284**:977–981.

13. Shimada, T., et al. 2001. Cloning and characterization of FGF23 as a causative factor of tumor-induced osteomalacia. *Proc. Natl. Acad. Sci. U. S. A.* **98**:6500–6505.

14. White, K.E., et al. 2001. The autosomal dominant hypophosphatemic rickets (ADHR) gene is a secreted polypeptide overexpressed by tumors that cause phosphate wasting. *J. Clin. Endocrinol. Metab.* **86**:497–500.

15. Larsson, T., et al. 2003. Immunohistochemical detection of FGF-23 protein in tumors that cause oncogenic osteomalacia. *Eur. J. Endocrinol.* **148**:269–276.

16. Saito, H., et al. 2003. Human fibroblast growth factor-23 mutants suppress Na+-dependent phosphate Co-transport activity and 1alpha,25-dihydroxyvitamin D3 production. *J. Biol. Chem.* **278**:2206–2211.

17. Shimada, T., et al. 2002. Mutant FGF-23 responsible for autosomal dominant hypophosphatemic rickets is resistant to proteolytic cleavage and causes hypophosphatemia in vivo. *Endocrinology.* **143**:3179–3182.

18. Bai, X., Miao, D., Goltzman, D., and Karaplis, A.C. 2003. The autosomal dominant hypophosphatemic rickets R176Q mutation in FGF-23 resists proteolytic cleavage and enhances in vivo biological potency. [Serial online.] **278**:9843–9849. http://www.jbc.org.

19. Yamazaki, Y., et al. 2002. Increased circulatory level of biologically active full-length FGF-23 in patients with hypophosphatemic rickets/osteomalacia. *J. Clin. Endocrinol. Metab.* **87**:4957–4960.

20. Jonsson, K.B., et al. 2003. Fibroblast growth factor 23 in oncogenic osteomalacia and X-linked hypophosphatemia. *N. Engl. J. Med.* **348**:1656–1663.

21. Jan de Beur, S.M., et al. 2002. Tumors associated with oncogenic osteomalacia express genes important in bone and mineral metabolism. *J. Bone Miner. Res.* **17**:1102–1110.

22. Ausubel, F. 2003. *Current protocols in molecular biology*. John Wiley & Sons. New York, New York, USA. 1.0.1–A.5.45.

23. Sambrook, J., and Russell, D.W. 2001. *Molecular cloning: A laboratory manual*. Cold Spring Harbor Laboratory Press. Plainview, New York, USA. 1.1–I.44.

24. Chen, P., Toribara, T., and Warnner, H. 1956. Microdetermination of phosphorus. *Anal. Chem.* **28**:1756–1758.

25. Führ J., Kazmarczyk, J., and Krüttgen C.D. 1955. Eine einfache colorimetrische Methode zur Inulin-Bestimmung für Nieren-clearanceuntersuchungen bei StoffwechselGesunden und Diabetikern. *Klin. Wochenschr.* **33**:729–730.

26. Nagubandi, S., Kumar, R., Londowski, J.M., Corradino, R.A., and Tietz, P.S. 1980. Role of vitamin D glucosiduronate in calcium homeostasis. *J. Clin. Invest.* **66**:1274–1280.

27. Nagubandi, S., Londowski, J.M., Bollman, S., Tietz, P., and Kumar, R. 1981. Synthesis and biological activity of vitamin D3 3 beta-sulfate. Role of vitamin D3 sulfates in calcium homeostasis. *J. Biol. Chem.* **256**:5536–5539.

28. Kumar, R., Nagubandi, S., Jardine, I., Londowski, J.M., and Bollman, S. 1981. The isolation and identification of 5,6-trans-25-hydroxyvitamin D3 from the plasma of rats dosed with vitamin D3. Evidence for a novel mechanism in the metabolism of vitamin D3. *J. Biol. Chem.* **256**:9389–9392.

29. Kumar, R., Londowski, J.M., Murari, M.P., and Nagubandi, S. 1982. Synthesis and biological activity of vitamin D2 3 beta-glucosiduronate and vitamin D2 3 beta-sulfate: role of vitamin D2 conjugates in calcium homeostasis. *J. Steroid Biochem.* **17**:495–502.

30. Coligan, J., Kruisbeek, A.M., Margulies, D.M., Shevach, E.M., and Strober, W. 2003. *Current protocols in immunology*. John Wiley & Sons. New York, New York, USA. 2.0.1–3.22.6

31. Laemmli, U.K. 1970. Cleavage of structural proteins during the assembly of the head of bacteriophage T4. *Nature.* **227**:680–685.

32. Towbin, H., Staehelin, T., and Gordon, J. 1979. Electrophoretic transfer of proteins from polyacrylamide gels to nitrocellulose sheets: procedure and some applications. *Proc. Natl. Acad. Sci. U. S. A.* **76**:4350–4354.

33. White, K.E., et al. 2001. The autosomal dominant hypophosphatemic rickets (ADHR) gene is a secreted polypeptide overexpressed by tumors that cause phosphate wasting. *J. Clin. Endocrinol. Metab.* **86**:497–500.

34. Drezner, M.K. 2000. PHEX gene and hypophosphatemia. *Kidney Int.* **57**:9–18.

35. Yamashita, T., Konishi, M., Miyake, A., Inui, K., and Itoh, N. 2002. Fibroblast growth factor (FGF)-23 inhibits renal phosphate reabsorption by activation of the mitogen-activated protein kinase pathway. *J. Biol. Chem.* **277**:28265–28270.

36. 1995. A gene (PEX) with homologies to endopeptidases is mutated in patients with X-linked hypophosphatemic rickets. The HYP Consortium. *Nat. Genet.* **11**:130–136.

37. Shimada, T., et al. 2001. Transgenic mice expressing fibroblast growth factor 23 (FGF23) demonstrate hypophosphatemia with low 1,25-dihydroxyvitamin D and rickets/osteomalacia. *J. Bone Miner. Res.* **16**(Suppl.):S151.

38. Shimada, T., et al. 2002. Targeted ablation of FGF-23 causes hyperphosphatemia, increased 1,25-dihydroxyvitamin D levels and severe growth retardation. *J. Bone Miner. Res.* **17**(Suppl):S168.

39. 2000. Autosomal dominant hypophosphataemic rickets is associated with mutations in FGF23. The ADHR Consortium. *Nat. Genet.* **26**:345–348.

40. White, K.E., et al. 2001. Autosomal-dominant hypophosphatemic rickets (ADHR) mutations stabilize FGF-23. *Kidney Int.* **60**:2079–2086.

41. Velculescu, V.E., Zhang, L., Vogelstein, B., and Kinzler, K.W. 1995. Serial analysis of gene expression. *Science.* **270**:484–487.

42. Velculescu, V.E., Vogelstein, B., and Kinzler, K.W. 2000. Analysing uncharted transcriptomes with SAGE. *Trends Genet.* **16**:423–425.

43. Berndt, T.J., and Knox, F.G. 1985. Nephron site of resistance to phosphaturic effect of PTH during respiratory alkalosis. *Am. J. Physiol.* **249**:F919–F922.

44. Berndt, T.J., and Knox, F.G. 1984. Proximal tubule site of inhibition of phosphate reabsorption by calcitonin. *Am. J. Physiol.* **246**:F927–F930.

45. Tanaka, Y., and Deluca, H.F. 1973. The control of 25-hydroxyvitamin D metabolism by inorganic phosphorus. *Arch. Biochem. Biophys.* **154**:566–574.

46. Tanaka, Y., and Deluca, H.F. 1974. Role of 1,25-dihydroxyvitamin D3 in maintaining serum phosphorus and curing rickets. *Proc. Natl. Acad. Sci. U. S. A.* **71**:1040–1044.

47. Tanaka, Y., Frank, H., and DeLuca, H.F. 1973. Intestinal calcium transport: stimulation by low phosphorus diets. *Science.* **181**:564–566.

48. Tanaka, Y., Frank, H., and DeLuca, H.F. 1973. Biological activity of 1,25-dihydroxyvitamin D3 in the rat. *Endocrinology.* **92**:417–422.

49. DeLuca, H.F., and Schnoes, H.K. 1976. Metabolism and mechanism of action of vitamin D. *Annu. Rev. Biochem.* **45**:631–666.

50. DeLuca, H.F., and Schnoes, H.K. 1983. Vitamin D: recent advances. *Annu. Rev. Biochem.* **52**:411–439.

51. Drezner, M.K. 1984. The role of abnormal vitamin D metabolism in X-linked hypophosphatemic rickets and osteomalacia. *Adv. Exp. Med. Biol.* **178**:399–404.

52. Biber, J., Hernando, N., Traebert, M., Volkl, H., and Murer, H. 2000. Parathyroid hormone-mediated regulation of renal phosphate reabsorption. *Nephrol. Dial. Transplant.* **15**:29–30.

53. Biber, J., Murer, H., and Forster, I. 1998. The renal type II Na+/phosphate cotransporter. *J. Bioenerg. Biomembr.* **30**:187–194.

54. Karim-Jimenez, Z., Hernando, N., Biber, J., and Murer, H. 2001. Molecular determinants for apical expression of the renal type IIa Na+/Picotransporter. *Pflugers Arch.* **442**:782–790.

55. Rattner, A., et al. 1997. A family of secreted proteins contains homology to the cysteine-rich ligand-binding domain of frizzled receptors. *Proc. Natl. Acad. Sci. U. S. A.* **94**:2859–2863.

56. Hoang, B., Moos, M., Jr., Vukicevic, S., and Luyten, F.P. 1996. Primary structure and tissue distribution of FRZB, a novel protein related to Drosophila frizzled, suggest a role in skeletal morphogenesis. *J. Biol. Chem.* **271**:26131–26137.

57. Zorn, A.M. 1997. Cell-cell signalling: frog frizbees. *Curr. Biol.* **7**:R501–R504.

58. Jones, S.E., and Jomary, C. 2002. Secreted Frizzled-related proteins: searching for relationships and patterns. *Bioessays.* **24**:811–820.

59. Dann, C.E., et al. 2001. Insights into Wnt binding and signalling from the structures of two Frizzled cysteine-rich domains. *Nature.* **412**:86–90.

60. Leyns, L., Bouwmeester, T., Kim, S.H., Piccolo, S., and De Robertis, E.M. 1997. Frzb-1 is a secreted antagonist of Wnt signaling expressed in the Spemann organizer. *Cell.* **88**:747–756.

61. Wang, S., Krinks, M., Lin, K., Luyten, F.P., and Moos, M., Jr. 1997. Frzb, a secreted protein expressed in the Spemann organizer, binds and inhibits Wnt-8. *Cell.* **88**:757–766.

62. Melkonyan, H.S., et al. 1997. SARPs: a family of secreted apoptosis-related proteins. *Proc. Natl. Acad. Sci. U. S. A.* **94**:13636–13641.

63. Mayr, T., et al. 1997. Fritz: a secreted frizzled-related protein that inhibits Wnt activity. *Mech. Dev.* **63**:109–125.

64. Hoang, B.H., et al. 1998. Expression pattern of two Frizzled-related genes, Frzb-1 and Sfrp-1, during mouse embryogenesis suggests a role for modulating action of Wnt family members. *Dev. Dyn.* **212**:364–372.

65. Finch, P.W., et al. 1997. Purification and molecular cloning of a secreted, frizzled-related antagonist of Wnt action. *Proc. Natl. Acad. Sci. U. S. A.* **94**:6770–6775.

66. Lin, K., et al. 1997. The cysteine-rich frizzled domain of Frzb-1 is required and sufficient for modulation of Wnt signaling. *Proc. Natl. Acad. Sci. U. S. A.* **94**:11196–11200.

67. Bafico, A., et al. 1999. Interaction of frizzled related protein (FRP) with Wnt ligands and the frizzled receptor suggests alternative mechanisms

for FRP inhibition of Wnt signaling. *J. Biol. Chem.* **274**:16180–16187.

68. Hsieh, J.C., Rattner, A., Smallwood, P.M., and Nathans, J. 1999. Biochemical characterization of Wnt-frizzled interactions using a soluble, biologically active vertebrate Wnt protein. *Proc. Natl. Acad. Sci. U. S. A.* **96**:3546–3551.

69. Nusse, R. 1992. The Wnt gene family in tumorigenesis and in normal development. *J. Steroid Biochem. Mol. Biol.* **43**:9–12.

70. Nguyen, H.T., Thomson, A.A., Kogan, B.A., Baskin, L.S., and Cunha, G.R. 1999. Expression of the Wnt gene family during late nephrogenesis and complete ureteral obstruction. *Lab. Invest.* **79**:647-658.

71. Nusse, R., and Varmus, H.E. 1992. Wnt genes. *Cell.* **69**:1073–1087.

72. Vainio, S.J., and Uusitalo, M.S. 2000. A road to kidney tubules via the Wnt pathway. *Pediatr. Nephrol.* **15**:151–156.

73. Vainio, S.J., Itaranta, P.V., Perasaari, J.P., and Uusitalo, M.S. 1999. Wnts as kidney tubule inducing factors. *Int. J. Dev. Biol.* **43**:419–423.

74. Sakanaka, C., Sun, T.Q., and Williams, L.T. 2000. New steps in the Wnt/beta-catenin signal transduction pathway. *Recent Prog. Horm. Res.* **55**:225–236.

75. Uusitalo, M., Heikkila, M., and Vainio, S. 1999. Molecular genetic studies of Wnt signaling in the mouse. *Exp. Cell Res.* **253**:336–348.

76. Povelones, M., and Nusse, R. 2002. Wnt signalling sees spots. *Nat. Cell Biol.* **4**:E249–E250.

77. Pandur, P., Lasche, M., Eisenberg, L.M., and Kuhl, M. 2002. Wnt-11 activation of a non-canonical Wnt signalling pathway is required for cardiogenesis. *Nature.* **418**:636–641.

78. Pandur, P., Maurus, D., and Kuhl, M. 2002. Increasingly complex: new players enter the Wnt signaling network. *Bioessays.* **24**:881–884.

79. Rattner, A., et al. 1997. A family of secreted proteins contains homology to the cysteine-rich ligand-binding domain of frizzled receptors. *Proc. Natl. Acad. Sci. U. S. A.* **94**:2859–2863.

80. Wolf, V., et al. 1997. DDC-4, an apoptosis-associated gene, is a secreted frizzled relative. *FEBS Lett.* **417**:385–389.

81. Bejsovec, A. 2000. Wnt signaling: An embarrassment of receptors. *Curr. Biol.* **10**:R919–R922.

82. Cadigan, K.M., and Nusse, R. 1997. Wnt signaling: a common theme in animal development. *Genes Dev.* **11**:3286–3305.

83. Dale, T.C. 1998. Signal transduction by the Wnt family of ligands. *Biochem. J.* **329**:209–223.

84. James, I.E., et al. 2000. FrzB-2: a human secreted frizzled-related protein with a potential role in chondrocyte apoptosis. *Osteoarthritis Cartilage.* **8**:452–463.

85. Schumann, H., Holtz, J., Zerkowski, H.R., and Hatzfeld, M. 2000. Expression of secreted frizzled related proteins 3 and 4 in human ventricular myocardium correlates with apoptosis related gene expression. *Cardiovasc. Res.* **45**:720–728.

86. Fujita, M., et al. 2002. Differential expression of secreted frizzled-related protein 4 in decidual cells during pregnancy. *J. Mol. Endocrinol.* **28**:213–223.

87. Wong, S.C., et al. 2002. Expression of frizzled-related protein and Wnt-signalling molecules in invasive human breast tumours. *J. Pathol.* **196**:145–153.

88. Leimeister, C., Bach, A., and Gessler, M. 1998. Developmental expression patterns of mouse sFRP genes encoding members of the secreted frizzled related protein family. *Mech. Dev.* **75**:29–42.